

Distributed Flexibility to Maintain Security Margin through Decentralised TSO-DSO Coordination

Saman Nikkhah^{a,*}, Abbas Rabiee^b, Alireza Soroudi^b, Adib Allahham^a, Philip C. Taylor^c, Damian Giaouris^a

^a*School of Engineering, Newcastle University, Newcastle upon Tyne, NE1 7RU, UK*

^b*School of Electrical and Electronic Engineering, University College Dublin, Dublin, Ireland*

^c*University of Bristol, Beacon House, Queens Road, Bristol BS8 1QU, UK*

Abstract

The increasing role of distribution networks as an active entity in the whole power and energy system, development of a unified power flow method to provide an integrated analysis of transmission and distribution networks becomes essential. Traditional methods have not addressed the challenge of voltage security in the coordination, while disconnecting the whole distribution network is considered as a solution for preventing major issues. This paper proposes a decentralised scheme for the coordination of transmission and distribution networks while maintaining the voltage security of the whole integrated system. At the transmission level, the transmission network operator (TSO) solves a centralised optimisation problem to minimise the system load curtailment while maintaining the system security margin. The TSO communicates the required set-points in the interface with distribution grids to the distribution system operators (DSOs.) At the distribution level, the DSOs utilise their available distributed flexibilities, such as conservation voltage reduction and feeder reconfiguration, to provide the required set-points and preserve the whole system security margin, with minimum load curtailment. This decentralised optimisation scheme preserves the system security with minimum information exchange between operators, as well as minimum physical load curtailment. The distributed flexibilities of all DSOs are utilised to meet the required security margin of the whole system. The proposed TSO-DSO coordination model is applied to the IEEE 118-bus transmission network, and the 83-bus practical distribution network of Taiwan Power Company and IEEE 33-bus feeder are considered as the connected distribution networks. The results show that the distributed flexibilities are capable of reducing the system demand to preserve the desired security margin, without any need for imposing direct load curtailment.

Keywords: TSO-DSO coordination, distributed flexibilities, security margin, feeder reconfiguration, voltage regulator.

Sets and Indices

\mathcal{B}_b	Set of distribution network buses.
\mathcal{B}_S	Set of distribution network substations.
Ω_b	Set of transmission system buses.
ψ	Index for voltage-dependent load model. $\psi \in \{\textit{residential}, \textit{commercial}, \textit{industrial}\}$ load model.
b, j	Index of transmission or distribution system buses.
d	Index of parallel distribution feeders connected to a specific transmission bus.
N_b	Total number of parallel distribution feeders connected to the b -th transmission bus.

*Corresponding author

Email address: s.nikkhah2@newcastle.ac.uk (Saman Nikkhah)

41 **Parameters**

42	$(\alpha/\beta)_{b,d}^\psi$	The active/reactive exponent of load type ψ at Bus b of the d -th parallel distribution bus b .
43		
44	$(\hat{P}/\hat{Q})_b^D$	Active/reactive power demand in b -th bus of transmission system at SLP.
45	$(\overline{p}/\overline{q})_{b,d}^D$	Initial active/reactive power demand of b -th bus in the d -th parallel distribution feeder.
46	$(g/b)_{bj,d}$	Conductance/susceptance of the line connecting buses b and j in the d -th parallel distribution feeder.
47		
48	$(kp/kq)_{b,d}^\psi$	Active/reactive power share of load type ψ at Bus b of the d -th parallel distribution bus.
49		
50	$(P/Q)_b^D$	Active/reactive power demand in b -th bus of transmission system at COP.
51	$(P/Q)_b^{G_{\max/\min}}$	Maximum/minimum limits of $(P/Q)_b^G$.
52	$(p/q)_{b,d}^{S_{\max/\min}}$	Maximum/minimum value of $(p/q)_{b,d}^S$.
53	$(p/q)_b^{LC,max}$	Maximum limit of $(p/q)_b^{LC}$.
54	$(Y/\phi)_{bj}$	Magnitude/angle of bj -th element of the transmission system's admittance matrix.
55	Λ_b^D	Increment rate of the transmission system load.
56	Λ_b^G	Increment rate of active power output of generation units.
57	λ_{des}	Desired loading margin.
58	$\bar{v}_{b,d}$	Initial voltage magnitude of b -th bus in the d -th parallel distribution feeder.
59	$\pi_{b,d}^{dg}$	Available DG output.
60	$\pi_{b,d}^{(p/q)}$	Active/reactive power share of d -th parallel feeder connected to the transmission Bus b .
61		
62	$i_{bj,d}^{\max}$	Maximum limit of $i_{bj,d}$.
63	S_{bj}^{\max}	Maximum limit of S_{bj} .
64	$V_b^{\max/\min}$	Maximum/minimum limits of V_b .
65	$v_{b,d}^{\max/\min}$	Maximum/minimum limits of $v_{b,d}$.
66	Variables	
67	$(\hat{P}/\hat{Q})_b^G$	Active/reactive power output of generation unit of Bus b at the SLP.
68	$(V/\theta)_b$	Voltage magnitude/angle of b -th bus of transmission system at the SLP.
69	$(P/Q)_b^G$	Active/reactive power output of generation unit of Bus b at the COP.
70	$(P/Q)_b^{LC}$	Active/reactive load curtailment at b -th transmission bus.
71	$(p/q)_{b,d}^S$	Active/reactive power injection at b -th bus of the d -th parallel distribution feeder.
72	$(p/q)_{b,d}^{dg}$	Active/reactive DG output.
73	$(p/q)_{bj,d}$	Active/reactive power flowing through the line connecting buses b and j in the d -th parallel distribution feeder.
74		
75	$(p/q)_b^{LC}$	Active/reactive load curtailment in the b -th bus in the d -th parallel distribution feeder.
76	$(V/\theta)_b$	Voltage magnitude/angle of b -th bus of transmission system at the COP.
77	$(v/\theta)_{b,d}$	Voltage magnitude/angle of b -th bus in the d -th parallel distribution feeder.
78	$\chi_{bj,d}^l$	Binary variable indicating the on/off status of line l connecting buses b and j in the d -th parallel distribution feeder.
79		
80	λ	Loading margin of the transmission network.
81	$\tau_{bj,d}$	Tap level of the voltage regulator on the line between buses b and j in the d -th parallel distribution feeder.
82		
83	$i_{bj,d}$	Current flowing through the line connecting buses b and j in the d -th parallel distribution feeder.
84		
85	S_{bj}/\hat{S}_{bj}	Power flow between transmission buses b and j at COP/SLP.

86 1. Introduction

87 Restructuring within the electricity power industry has created opportunities for small businesses,
88 enabling more competition and possibly ending electricity market monopolies. It has also enabled
89 the engagement of distribution system operators (DSOs) in the energy markets. Despite substantial
90 opportunities created by this new paradigm, the lack of sufficient coordination between transmission
91 system operator (TSO) and DSOs can create critical challenges, especially during an emergency con-
92 dition (e.g. sudden changes in the system load or generation failure) in the network. The UK power
93 outage in 2019 can be an example of lack of TSO-DSO coordination, where millions of customers at
94 the distribution level were disconnected from the main grid by under-frequency load shedding [1].

95 This event highlights the necessity of cooperation between TSO and DSOs. The cooperation be-
96 tween operators can enable a coordinated control architecture in the whole network [2]. Although a
97 coordinated scheme allows the DSOs to have a direct role in the market, in practice, TSOs are still
98 responsible for the secure operation of the whole system [3]. Consequently, under emergency condi-
99 tions, TSOs can disconnect the distribution feeders and all of their connected loads to preserve system
100 security. This, however, can bring about significant techno-economic losses to the system managers.
101 Therefore, system security is a challenge that questions the effectiveness of available TSO-DSO co-
102 ordination models [4]. A practical coordinated framework should enable flexibility in the DSOs to
103 preserve system security. This raises an important question (recently considered in the Global Power
104 System Transformation Consortium’s Research Agenda Group) [5]: *“How can grid topology be flexi-
105 bly adapted to various operating conditions?”*

106 In the literature, network flexibility is mainly achieved through optimal management of different
107 types of distributed energy resources (DERs) at the distribution system level. In [6], a reserve provi-
108 sion capability method is utilised for estimating the reserve requirement of TSOs and the capability of
109 DSOs in complying with the upper-level needs. This proposed model is solved for a planning stage,
110 however, it has not considered the sudden changes in the operation of the coordinated system. The
111 capability of distribution networks in providing reactive power support for the transmission system is
112 studied in [7], where intermittency of renewable distributed generation units is considered, with the
113 authors proposing a capability chart for investigating the effect of uncertainty on the service provision.
114 In [8], the influence of local markets on the TSO-DSO coordination is investigated with a bi-level op-
115 timisation problem considering the conflicting objectives. The results show that both TSOs and DSOs
116 should consider a budget to be robust in face of renewable power generation uncertainty. Reference [9]
117 proposed a real-time energy management strategy for distribution systems, analysing various flexibility
118 services that could be provided for the transmission level in the interface of these networks.

119 The cooperation between transmission and distribution systems is subjected to several technical
120 and operational challenges, which have been summarised in [3]. These aspects can also affect the
121 policies of cooperation. Each entity has its own objectives. For example, TSOs might aim to minimise
122 their costs. DSOs focus on addressing the reliability of load supply. These different objectives create a
123 substantial challenge in terms of information exchange privacy [10]. A decentralised control approach
124 could address this coordination challenge. A decentralised coordination scheme for distributed gener-
125 ation units is proposed in [11] to meet the reactive power set-points of the TSO-DSO interface, with
126 the aim of minimising the power losses while satisfying the distribution grid constraints. The authors
127 also proposed a control scheme for on-load tap changer so as to unlock higher level of reactive power
128 flexibility. A market clearing framework is proposed in [12] for trading the flexibility provided by the
129 distributed generation in the distribution level. The results show that the flexibility in the distribution
130 level can affect the locational marginal prices in the transmission level. A decentralised control model
131 is introduced in [13], where the DSO and TSO solve their own optimisation and balance the reactive

Table 1
Taxonomy of control models in TSO-DSO coordination literature.

Ref. No	Flexibility measure				Control method		Power flow constraints		
	DER	Reconfiguration	CVR	load	Centralised	Decentralised	Transmission network	Distribution network	Voltage stability
[6, 7, 9, 22]	✓	x	x	x	✓	x	x	✓	x
[8, 13, 15, 17]	✓	x	x	x	x	✓	✓	✓	x
[11, 14]	✓	x	x	x	x	✓	x	✓	x
[12]	✓	x	x	✓	x	✓	✓	✓	x
[21]	✓	x	x	x	x	✓	✓	✓	x
[23]	✓	x	x	x	✓	x	✓	✓	x
[24, 25]	✓	x	x	✓	✓	x	x	✓	x
This study	✓	✓	✓	x	x	✓	✓	✓	✓

132 power in their interface. This iterative approach in coordination is also utilised in [14]. Yuan *et al.* [15]
133 proposed a hierarchical coordination approach based on the economic dispatch, where DSOs solve
134 their optimisation at an upper level and report the solution to the TSOs. The final solution is achieved
135 in an iterated manner. Considering the high rate of (R/X) in the distribution systems, however, a simple
136 economic dispatch or a DC-OPF cannot reflect the operational and dynamic characteristics of the
137 network [16]. In [17], a diagonal quadratic approximation method is utilised for coordinating the OPF
138 problems of the TSOs and DSOs. The security of the coordination with the least information exchange
139 remains a challenge in available methodologies.

140 Preserving the integrated system security is a challenging issue of the coordination [18]. An im-
141 portant indicator for evaluating system security is the voltage stability margin [19, 20]. Therefore,
142 voltage stability assessment has been followed by researchers to evaluate the security of TSO-DSO
143 coordination. A joint static voltage stability analysis is introduced in [21] for evaluating the security
144 of integrated distribution and transmission systems. In [22], voltage stability requirement is translated
145 into the need for reactive power and a methodology is proposed to defer investment in reactive power
146 compensation equipment while satisfying the required margin through optimal control of synchronous
147 and non-synchronous generation units. The impact of DER technologies installed in the distribution
148 level is shown by the authors. Tang *et al.* [23] compared the accuracy of data-driven methods with the
149 OPF-based models in the coordination of TSO and DSOs. The positive role of flexibility services, pro-
150 vided by the distribution networks, on the heavily loaded buses of the transmission network is shown
151 in [24]. The dynamics of the distribution system are neglected and the evaluation of transmission
152 contingency analysis is performed based on the forecasted load and generation. In [25], the role of
153 distribution network in providing the voltage support for the transmission level is studied in a real-time
154 centralised optimisation method. A model-free framework is introduced in [26] for exploiting the flex-
155 ibility provided by the low-voltage level DERs in order to provided voltage support both in normal and
156 emergence condition for the transmission network. Reference [27] proposed a security constrained
157 unit commitment for TSO-DSO coordination with the aim of reducing the computational time. In an
158 emergency condition, however, the objective functions of system operators would focus on secure op-
159 eration of the system rather than a cost-optimal unit commitment. The main challenge that remains,
160 however, is how to introduce security measures as critical components of TSO-DSO coordination.

161 Although the coordination between TSOs and DSOs has been studied before, the amount of data
162 exchange, distribution system flexibility, and system security are three important considerations that
163 need more investigation.

- 164 1. With increasing the numbers of distribution systems connected to a transmission network, it is
165 important to reduce the volume of data exchange. This can help in optimising TSO problems
166 with short computational time. Therefore, an efficient method that solves the optimisation on

167 both sides with the least information exchange and while preserving the system security needs
168 to be developed.

169 2. The study of distribution system flexibility focuses mainly on the potential of distributed genera-
170 tion to provide services for the upper network in a normal situation. Nevertheless, there are other
171 practical methods that should be studied for evaluating the distribution level flexibility under dif-
172 ferent circumstances including an emergency condition (e.g. conservation voltage reduction and
173 network reconfiguration).

174 3. Although voltage stability analysis has been studied to evaluate the security of TSO-DSO coor-
175 dination, it is not considered a critical constraint in designing decentralised optimisation models.
176 This security measure should be added to the OPF model of decentralised optimisations of TSO
177 and DSO. Such a scheme should highlight the importance of DSOs in preserving the security of
178 TSO-DSO coordination.

179 This study aims at addressing these challenges by introducing a decentralised security-constrained
180 TSO-DSO coordination framework. The proposed method investigates the practical flexibility options
181 at the distribution level for preventing load curtailment in an emergency condition. A decentralised
182 control architecture is proposed for optimising the critical components of the power flow model (i.e.
183 active/reactive power, and voltage magnitude) in the interface between transmission and distribution
184 networks. Rather than consider models of frise coordination, this method is designed to achieve op-
185 timal values in the boundary points connecting the transmission and distribution networks. To ensure
186 secure coordination, the proposed model considers the loading margin as the security measure. This
187 measure should be satisfied under different circumstances. The TSO optimises the system operation
188 while preserving the system security. The desired values of power exchange and voltage level in the
189 interface are sent to the DSOs. To respond to the required set-point given by the TSO, the distributed
190 DSO optimisers try to benefit from available network flexibility options while respecting the integrity
191 of their internal constraints. The first promising flexibility option is the use of voltage regulators in the
192 distribution level, as the demands are voltage-dependent. This scheme is widely known as conservation
193 voltage reduction (CVR) [28]. The next network flexibility option is the reconfiguration of the distribu-
194 tion network, which has been used to improve different techno-economic characteristics of distribution
195 grid separately [29]. The solutions of DSO optimisers are sent to the interface and compared with the
196 requirement of TSO. This process is repeated by optimisers until a degree of convergence is achieved.
197 If the DSOs fail in satisfying the required boundary points, they would apply the load curtailment to
198 preserve the security of the whole system. This paradigm highlights the role of DSOs in providing
199 flexibility measures for preserving the TSO-DSO coordination. This framework can converge with a
200 small number of iterations and with a short computational time (only seconds), which enables it as a
201 suitable practical TSO-DSO coordination scheme for research and industry. The main contributions of
202 this paper are:

203 • A decentralised control framework is introduced for TSO-DSO coordination with the least in-
204 formation exchange between them. In this method, DSOs use their available flexibility measures
205 or/and load curtailment to comply with the requirements of the TSO. This proposed method ben-
206 efits from short computational time spans and achieves the required convergence degree with a
207 small number of iterations.

208 • Distributed optimal conservation voltage reduction and network reconfiguration are adopted as
209 the flexibility measures preserving the security of TSO-DSO coordination with minimum phys-
210 ical load curtailment. In the upper level, the TSO ensures the minimum loading margin for the

211 transmission network considering the critical components of the power flow model. In the lower-
212 level distributed optimisation models, DSOs aim at minimising the actual load curtailment, using
213 the available flexibility options. Each DSO provides a different level of flexibility in the proposed
214 distributed framework. However, the total flexibility provided comply with the requirements of
215 the TSO.

- 216 • The transmission network's loadability constraint is considered as the main security margin in-
217 fluencing the TSO-DSO coordination. This index can be utilised as a measure for evaluating the
218 degree of security of TSO-DSO coordination.

219 The remainder of this paper is organised as follows: Section 2 explains the framework of the
220 proposed TSO-DSO coordination. Mathematical formulation is introduced in Section 3. Section 4
221 explains the solving process of the decentralised optimisation approach. The simulation results are
222 given in Section 5. Finally Section 6 concludes the paper.

223 2. Framework Description

224 A visualisation of the proposed TSO-DSO coordination framework is presented in Fig. 1. This
225 framework is suggested for a known number of parallel distribution feeders that are connected to a
226 transmission network in the interface of these networks. Based on this architecture, an optimisation
227 problem is first solved by the TSO. Since voltage stability is an important security criterion in the
228 cooperation between TSO and DSO [21], it can be considered as the main influence on the coordination
229 between networks. Accordingly, the optimisation in the transmission level always considers a degree
230 of loading margin (i.e. security margin) as an important constraint of the model. This is shown in the
231 upper left-hand side of Fig. 1. In this regard, a sudden change in the system load (e.g. increasing above
232 the generation capacity) can create security issues for the TSO if the aim is to keep the loading margin
233 in the preferred range.

234 In a conventional TSO-DSO coordination scheme, the TSO optimiser is more likely to apply load
235 curtailment to some heavily loaded buses which are connected to the lower-level distribution grids.
236 However, TSOs can benefit from the flexibility measures in the distribution networks. The method-
237 ology designed in this paper highlight the role of the flexibility measures in the distribution networks
238 for preserving the system security. Therefore, the outcomes of the TSO optimiser in the point of con-
239 nection with the distribution grids are sent to the distributed DSO optimisers. These values are shown
240 with $U_{1..n}^{TSO}$ in Fig. 1. Each DSO compiles its distributed optimisation based on the received data. To
241 prevent load curtailment, DSOs try to utilise the available flexibility options in the distribution level
242 to comply with the requirements of the TSO. To do so, they utilise the CVR to adjust voltage within
243 the permissible range which can result in load reduction. Simultaneously with this strategy, the DSOs
244 adopt the network reconfiguration to decrease the power loss and improve the voltage profile. After
245 applying these strategies to the distribution network via an optimisation model, the DSOs compare the
246 preferred values (i.e. $U_{1..n}^{DSO}$) with those received from the TSO. If the values are lower than that of the
247 TSO, they are sent to the TSO optimiser for another round of optimisation. This process is repeated
248 until the DSO values are equal or bigger than those of the TSO. The DSOs would apply load curtail-
249 ment if they cannot decrease their load level to preserve the security of coordination. The proposed
250 method converges in a small number of iterations and respects data privacy by considering only critical
251 components of the power flow model in the interface of the networks.

252 It is worth mentioning that this framework investigates the role of distributed flexibilities in TSO-
253 DSO coordination while complying with the security margin. Therefore, it does not address the sizing
254 of distribution networks. The number of distribution networks is assumed as a known parameter. In the

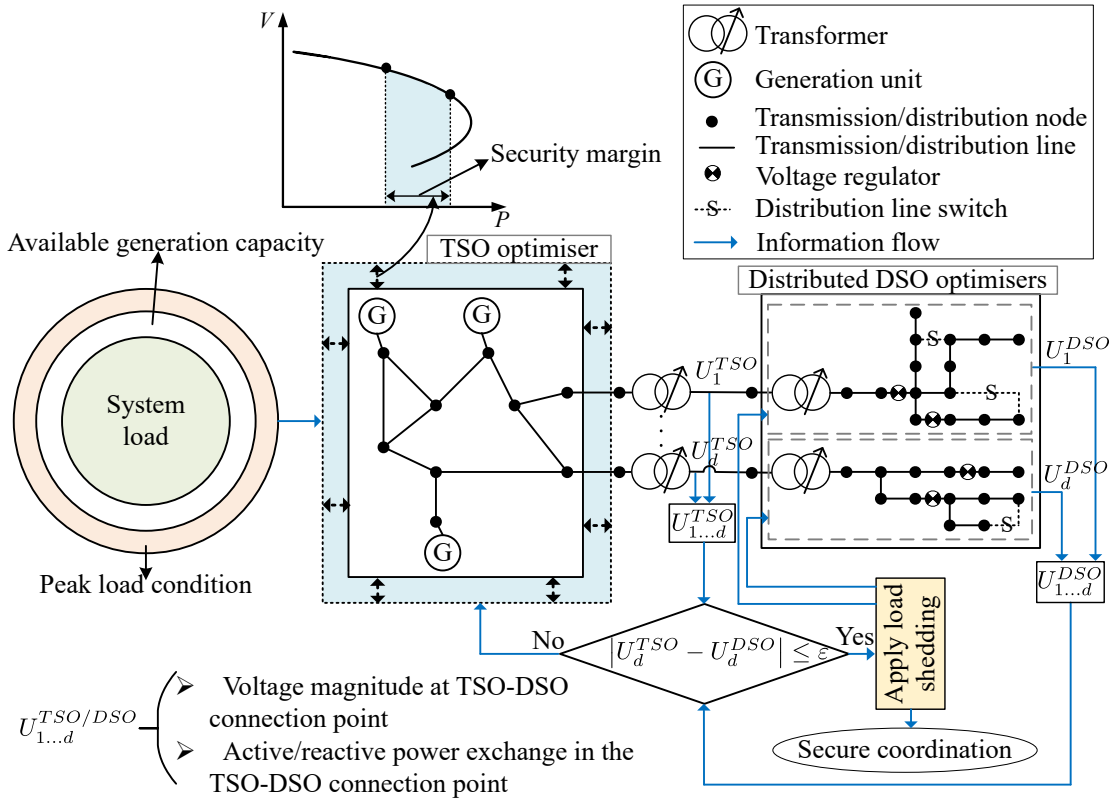


Figure 1: Conceptual illustration of the proposed architecture.

255 meantime, sensitivity analysis has been performed to show the variation of the results over the changes
 256 in the number of distribution networks.

257 3. Formulation of the Proposed TSO-DSO Coordination Framework

258 The proposed formulation for the decentralised control method is illustrated in Fig. 1. At the
 259 transmission level, the optimisation is solved with the aim of minimising the load curtailment under a
 260 peak loading condition while satisfying the required loading margin (i.e. security margin). The desired
 261 solutions of the optimisation in the connection point with the distribution networks are reported to the
 262 DSOs. The distributed DSO optimisers then utilise their available flexibility options to minimise the
 263 value of load curtailment and the difference between their required decision variables in the point of
 264 connection with the upper network. The following subsections express the mathematical model of the
 265 optimisation at each level.

266 3.1. TSO Centralised Optimiser

267 At the transmission network level, the TSO optimiser aims at minimising load curtailment and
 268 the difference between set-points in the interface with the distribution networks under a peak loading
 269 condition (i.e. emergency condition) while satisfying the operational and security constraints.

270 3.1.1. Objective function

271 The objective function of the TSO is given below:

$$OF^{TSO} = \min \{w_1 \times of_{lc}^{tso} + (1 - w_1) \times of_{dif}^{tso}\} \quad (1)$$

$$of_{lc}^{tso} = \sum_{b \in \Omega_b} P_b^{LC} \quad (2)$$

$$of_{dif}^{tso} = \sum_{b \in \Omega_b} \left(\left| (P_b^D - P_b^{LC}) - p_b^{I_{dso}} \right| + \left| (Q_b^D - Q_b^{LC}) - q_b^{I_{dso}} \right| + \left| V_b - v_b^{I_{dso}} \right| \right) \quad (3)$$

Equation (2) represents the load curtailment in the transmission system, while Eq. (3) is the difference between the set-points in the interface with the distribution networks.

3.1.2. Power flow and network constraints

Concerning the security of the system, it is necessary to consider the current operation power flow constraints in the transmission level simultaneously with those of the security limit point (SLP). This level also contains physical and operational constraints of the transmission grid (e.g., voltage magnitude/angle). The power flow and network constraints at the current operation point (COP) of the network are presented as below ($\forall b, j \in \Omega_b$):

$$P_b^G + P_b^{LC} - P_b^D = V_b \sum_{j \in \Omega_b} V_j Y_{bj} \cos(\theta_b - \theta_j - \phi_{bj}) \quad (4)$$

$$Q_b^G + Q_b^{LC} - Q_b^D = V_b \sum_{j \in \Omega_b} V_j Y_{bj} \sin(\theta_b - \theta_j - \phi_{bj}) \quad (5)$$

$$P_b^{G_{min}} \leq P_b^G \leq P_b^{G_{max}} \quad (6)$$

$$Q_b^{G_{min}} \leq Q_b^G \leq Q_b^{G_{max}} \quad (7)$$

$$0 \leq P_b^{LC} \leq P_b^{LC, max} \quad (8)$$

$$0 \leq Q_b^{LC} \leq Q_b^{LC, max} \quad (9)$$

$$V_b^{min} \leq V_b \leq V_b^{max} \quad (10)$$

$$-S_{bj}^{max} \leq S_{bj} \leq +S_{bj}^{max} \quad (11)$$

Constraints (4) and (5) are active and reactive power flow at the COP respectively; constraints (6) and (7) limit the upper and lower capacity of generation units respectively; constraints (8)-(9) show the limits on the load curtailments. Constraint (10) represents the limits on the voltage magnitude of system buses; constraint (11) shows the the transmission line capacity.

3.1.3. Security constraints

Due to the importance of security measures in the TSO-DSO coordination, they are considered as the critical component of the OPF model in the TSO optimisation. To do so, as shown in the top left corner of Fig. 1, the loading margin is considered as the security measure of TSO-DSO coordination. This security margin is defined by generation capacity requirements to supply rises in the system demand prior to the violation of SLP [30]. In the P-V curve shown in Fig. 1, the distance from point A (i.e. COP) to point B (i.e. SLP) is the loading margin (i.e. security margin). This margin is defined by the system load. For example, increasing the system demand from P_{D_0} (i.e. point A) to P (i.e. point

292 B) leads to a violation of the operational constraints of the network. Consequently, the system loading
 293 margin should be more than/equa to the preset level to keep the entire network in a secure operational
 294 state. In order to address this concept, the power flow equations in COP (i.e. (4)-(9)) should be
 295 simultaneously considered along with those of SLP, which are represented as below ($\forall b, j \in \Omega_b$):

$$\hat{P}_b^G - \hat{P}_b^D = \hat{V}_b \sum_{j \in \Omega_b} \hat{V}_j Y_{bj} \cos(\hat{\theta}_b - \hat{\theta}_j - \phi_{bj}) \quad (12)$$

$$\hat{Q}_b^G - \hat{Q}_b^D = \hat{V}_b \sum_{j \in \Omega_b} \hat{V}_j Y_{bj} \sin(\hat{\theta}_b - \hat{\theta}_j - \phi_{bj}) \quad (13)$$

$$P_b^{G_{\min}} \leq \hat{P}_b^G \leq P_b^{G_{\max}} \quad (14)$$

$$Q_b^{G_{\min}} \leq \hat{Q}_b^G \leq Q_b^{G_{\max}} \quad (15)$$

$$V_b^{\min} \leq \hat{V}_b \leq V_b^{\max} \quad (16)$$

$$-S_{bj}^{\max} \leq \hat{S}_{bj} \leq +S_{bj}^{\max} \quad (17)$$

$$\hat{P}_b^D = (1 + \Lambda_b^D \times \lambda) (P_b^D - P_b^{LC}) \quad (18)$$

$$\hat{Q}_b^D = (1 + \Lambda_b^D \times \lambda) (Q_b^D - Q_b^{LC}) \quad (19)$$

$$\hat{P}_b^G = \min (P_b^{G_{\max}}, (1 + \Lambda_g^G \times \lambda) P_g^G) \quad (20)$$

$$\hat{V}_b = V_b + v_b^l - v_b^u \quad (21)$$

$$(Q_b^{G_{\max}} - \hat{Q}_b^G) \times v_b^u \leq 0 \quad (22)$$

$$(\hat{Q}_b^G - Q_b^{G_{\max}}) \times v_b^l \leq 0 \quad (23)$$

$$v_b^l, v_b^u \geq 0 \quad (24)$$

$$\lambda \geq \lambda_{des} > 0 \quad (25)$$

296 where constraints (12) and (13) represent the active and reactive power flow at SLP respectively; limit
 297 on active and reactive power, voltage magnitude, and transmission line capacity at SLP are shown by
 298 constraints (14)-(17) respectively. The amount of increase in the active and reactive system demand
 299 from COP to the SLP is shown by (18) and (19) respectively. This increase in the system demand
 300 should be supplied by generation units, as represented by Equation (20). Constraints (21)-(24) describe
 301 the dynamics of load increase from COP to the SLP and the way it would affect the voltage at the
 302 system buses. Finally, the desired loading margin of the system can be defined by Constraint (25).

303 The net load seen in the interface of TSO and DSO is a key parameter that determines the secu-
 304 rity margin in the transmission network. This load is characterised by its active and reactive power
 305 components. The DSO is responsible to govern this demand, and in the proposed TSO-DSO coordi-
 306 nation approach, the DSO tries to manage the demand profile in the interface of TSO and DSO, by the
 307 available options such as VRs, network reconfiguration, and DERs.

308 The defined security margin in Eq. (25), is a unique parameter for the entire system, as in reality,
 309 when the system is pushed toward its loadability limit, the demand in almost all buses tends to increase.
 310 The load increment pattern in different buses may not be the same, and one can consider different load
 311 increment patterns in Eqs. (18) and (19), by considering different values for Λ_b^D . But, as from the
 312 security perspective, the worst load increment pattern is increasing both active and reactive powers
 313 simultaneously, in this paper a constant power factor increment pattern is considered for all buses.

314 By solving the above optimisation model for the TSO, the required load curtailment and voltage
 315 level at the interface of TSO-DSO are obtained. The following parameters will be determined:

$$\begin{bmatrix} P_b^{I_{tso}} \\ Q_b^{I_{tso}} \\ V_b^{I_{tso}} \end{bmatrix} = \begin{bmatrix} P_b^D - P_b^{LC} \\ Q_b^D - Q_b^{LC} \\ V_b \end{bmatrix} \quad (26)$$

316 The active and reactive power shares (i.e., $\pi_{b,d}^p$ and $\pi_{b,d}^q$) of d -th downstream feeder in the DSO's
 317 overall demand at the boundary point with the TSO (i.e. at bus b) is a known parameter for the DSO,
 318 which can be expressed as follows:

$$p_{b,d}^{I_{dso}} = \pi_{b,d}^p \times P_b^{I_{tso}} \quad (27)$$

$$\sum_d^{N_b} \pi_{b,d}^p = 1 \quad (28)$$

$$q_{b,d}^{I_{dso}} = \pi_{b,d}^q \times Q_b^{I_{tso}} \quad (29)$$

$$\sum_d^{N_b} \pi_{b,d}^q = 1 \quad (30)$$

319 3.2. Distributed DSO optimisers

320 After receiving the set-points required by the TSO at the TSO-DSO interface, a set of distributed
 321 optimisation models are solved in the distribution level to comply with the TSO's set-points, with
 322 minimum actual load curtailment, as the demands are mainly connected to the distribution level. In
 323 the distribution level optimisation model, the DSOs aim at minimising the physical load curtailment
 324 required by the TSO, via optimal coordination of distribution-level flexibilities. In this paper, network
 325 reconfiguration and CVR are considered as the DSO flexibility options. By optimising the distribution
 326 network topology via feeder reconfiguration, power losses and voltage profile of the network can be
 327 modified to achieve the DSO goals. Moreover, since the demand connected to the distribution feeder
 328 is mainly voltage-dependent, CVR can be considered as an effective flexibility option for DSOs. To
 329 implement CVR, coordinated operation of voltage regulators (i.e. boosting transformers) along the
 330 feeders can be utilised. The system demand can be modified through the coordinated operation of volt-
 331 age regulator transformers. In the following, the distributed optimisation model for DSOs is presented,
 332 taking into account the network reconfiguration and voltage regulators' flexibilities.
 333

334 3.2.1. Objective function

In the distribution level, each grid's optimiser tries to minimise the load curtailment and the dif-
 ference between its set-points in the TSO-DSO connection point with those obtained by the TSO's
 centralised optimiser, as below:

$$OF^{DSO} = \min \{w_2 \times of_{lc}^{dso} + (1 - w_2) \times of_{dif}^{dso}\} \quad (31)$$

$$of_{lc}^{dso} = \sum_{b \in B_b} p_{b,d}^{lc} \quad (32)$$

$$of_{dif}^{dso} = \sum_{b \in B_s} \left(\left| p_{b,d}^S - p_{b,d}^{I_{dso}} \right| + \left| q_{b,d}^S - q_{b,d}^{I_{dso}} \right| + \left| v_{b,d} - V_b^{I_{tso}} \right| \right) \quad (33)$$

335 where w_2 is a weight coefficient defining the importance of each objective in the distribution level
 336 optimisers.

337 **3.2.2. Power Flow and Network Constraints**

In this study, the power flow constraints in the distribution level are adopted by adding two important flexibility measures: network reconfiguration and CVR. The former adds a binary variable to the branch flow model and the voltage-dependent loads are considered for the latter. The power flow constraints in the distribution level are represented as below ($\forall b, j \in \mathcal{B}_b$):

$$p_{b,d}^S + p_{b,d}^{LC} - p_{b,d}^D = \sum_{j \in \mathcal{B}_b} \chi_{bj,d}^l \times p_{bj,d} \quad (34)$$

$$q_{b,d}^S + q_{b,d}^{LC} - q_{b,d}^D = \sum_{j \in \mathcal{B}_b} \chi_{bj,d}^l \times q_{bj,d} \quad (35)$$

$$p_{bj,d} = +g_{bj,d} \tau_{bj,d}^2 v_{b,d}^2 - \tau_{bj,d} v_{b,d} v_{j,d} (g_{bj,d} \cos(\theta_{bj,d}) + b_{bj,d} \sin(\theta_{bj,d})) \quad (36)$$

$$q_{bj,d} = -b_{bj,d} \tau_{bj,d}^2 v_{b,d}^2 - \tau_{bj,d} v_{b,d} v_{j,d} (g_{bj,d} \sin(\theta_{bj,d}) - b_{bj,d} \cos(\theta_{bj,d})) \quad (37)$$

$$p_{b,d}^D = \hat{p}_{b,d}^D \sum_{\psi} k p_{b,d}^{\psi} \left(\frac{v_{b,d}}{\hat{v}_{b,d}} \right)^{\alpha_{b,d}^{\psi}} \quad (38)$$

$$q_{b,d}^D = \hat{q}_{b,d}^D \sum_{\psi} k q_{b,d}^{\psi} \left(\frac{v_{b,d}}{\hat{v}_{b,d}} \right)^{\beta_{b,d}^{\psi}} \quad (39)$$

$$p_{b,d}^{S_{\min}} \leq p_{b,d}^S \leq p_{b,d}^{S_{\max}}, \quad \forall b \in \mathcal{B}_S \quad (40)$$

$$q_{b,d}^{S_{\min}} \leq q_{b,d}^S \leq q_{b,d}^{S_{\max}}, \quad \forall b \in \mathcal{B}_S \quad (41)$$

$$0 \leq p_{b,d}^{LC} \leq p_{b,d}^{LC,max} \quad (42)$$

$$0 \leq q_{b,d}^{LC} \leq q_{b,d}^{LC,max} \quad (43)$$

$$v_{b,d}^{\min} \leq v_{b,d} \leq v_{b,d}^{\max} \quad (44)$$

$$(v_{b,d} \times i_{bj,d})^2 = p_{bj,d}^2 + q_{bj,d}^2 \quad (45)$$

$$0 \leq i_{bj,d} \leq \chi_{bj,d}^l \times i_{bj,d}^{\max} \quad (46)$$

338 where constraints (34) and (35) represent the active and reactive power balance in the distribution net-
 339 work respectively. Constraints (36) and (37) show the active and reactive power flow in the distribution
 340 network respectively. Binary variable $\chi_{bj,d}^l$ indicates the status of line connecting the distribution buses
 341 b and j . Due to the fact that the majority of loads in the distribution level are voltage-dependent, the
 342 exponential load model for active and reactive loads are considered in equations (38) and (39) respec-
 343 tively. In these equations, it is assumed that the load in each distribution bus b , comprises of residential,
 344 commercial and industrial components. Constraints (40) and (41) respectively limit the active and re-
 345 active power imported from the transmission network to the distribution network from the substation
 346 bus. Constraints (42) and (43) limit the active and reactive load curtailment in the distribution network
 347 respectively. The voltage magnitude of system buses is limited by Constraint (44). Finally, the power
 348 flow through the distribution system lines is represented by (45) and limited by constraint (47).

349 **3.2.3. DER flexibility**

350 Distribution-level DERs can play a vital role in providing flexibility for the transmission network
 351 [11]. In order to unlock higher levels of flexibility, the network reconfiguration and CVR can be used

352 along with DER. To do so, active and reactive power output of DERs are added to the power balance
 353 equations in constraints (34) and (35), as below:

$$p_{b,d}^S + p_{b,d}^{dg} + p_{b,d}^{LC} - p_{b,d}^D = \sum_{j \in \mathcal{B}_b} \chi_{bj,d}^l \times p_{bj,d} \quad (47)$$

$$q_{b,d}^S + q_{b,d}^{dg} + q_{b,d}^{LC} - q_{b,d}^D = \sum_{j \in \mathcal{B}_b} \chi_{bj,d}^l \times q_{bj,d} \quad (48)$$

$$0 \leq p_{b,d}^{dg} \leq \pi_{b,d}^{dg} \quad (49)$$

$$-tg(\varphi_{lead}) \times P_{b,d}^{dg} \leq Q_{b,d}^{dg} \leq tg(\varphi_{lag}) \times P_{b,d}^{dg} \quad (50)$$

354 where constraints (47) and (48) represent the active and reactive power balance equations with consid-
 355 eration for active and reactive power output of DG units respectively. Constraint (49) represents the
 356 active power output of DG units based on their available capacity. Finally, Constraint (50) limits the
 357 reactive power output of DGs.

358 3.2.4. Distribution network's radiality constraints

359 Network reconfiguration is considered as one of the more efficient methods in improving system
 360 characteristics [31]. This method has been utilized to improve different aspects of the network includ-
 361 ing voltage profile. Therefore, it can be adopted to improve the distribution system voltage profile
 362 when the substation voltage level is reduced to save energy. In this study, the network reconfiguration
 363 is modeled based on the graph theory. Accordingly, to have a radial configuration, the number of dis-
 364 tribution lines should be equal to the number of nodes minus one. This concept can be mathematically
 365 modelled as below [32] ($\forall b, j \in \mathcal{B}_b$):

$$s_{b,d} - d_{b,d} = \sum_{(bj) \in \Omega_l} f_{bj,d} - \sum_{(jb) \in \Omega_l} f_{jb,d} \quad (51)$$

$$f_{bj,d} + f_{jb,d} = 0 \quad (52)$$

$$|f_{bj,d}| \leq \chi_{bj,d}^l f_{bj,d}^{max} \quad (53)$$

$$0 \leq s_{b,d} \leq s_{b,d}^{max}, \quad \forall b \in \mathcal{B}_S \quad (54)$$

$$\sum_{(bj) \in \mathcal{B}_b} \chi_{bj,d}^l = 2 \times (\text{card}(\mathcal{B}_b) - 1) \quad (55)$$

$$\chi_{bj,d}^l = \chi_{jb,d}^l \quad (56)$$

366 where $\chi_{bj,d}^l$ is a binary variable indicating the status of lines. It is equal to one if the circuit is closed
 367 and 0, otherwise. Combining (51) and (55) ensures that there is a path to every node and the graph
 368 connectivity is ensured. Therefore, in the proposed model for the distribution system, in addition to
 369 constraints (55) and (56), there is a need to have a path from the substation to all system loads, which
 370 has been reflected in equations (34) and (35).

371 By solving this, the model will determine the distributed DSO optimizers, the realized load ab-
 372 sorbed by the downstream distribution networks, as well as the optimal voltage at the interface point
 373 of TSO-DSO. Usually, several distribution feeders are supplied on the downstream side of a given in-
 374 terface point of the TSO-DSO. Therefore, the DSO aggregates the obtained load of all parallel feeders
 375 as follows:

$$\begin{bmatrix} p_b^{I_{dso}} \\ q_b^{I_{dso}} \\ v_b^{I_{dso}} \end{bmatrix} = \begin{bmatrix} \sum_{d=1}^{N_b} p_{b,d}^S \\ \sum_{d=1}^{N_b} q_{b,d}^S \\ \frac{1}{N_b} \sum_{d=1}^{N_b} v_{b,d} \end{bmatrix} \quad (57)$$

376 4. TSO-DSO Coordination Procedure

377 At the connection bus between transmission and the downstream distribution networks, the bound-
 378 ary variables including voltage magnitude, active and reactive power are obtained via the above opti-
 379 mization models. The vector of these boundary variables should converge to the same values for both
 380 the TSO and DSO optimizations. Hence, the convergence condition is as follows:

$$\begin{bmatrix} \epsilon_p \\ \epsilon_q \\ \epsilon_v \end{bmatrix} = \begin{bmatrix} |P_b^{I_{tso}} - p_b^{I_{dso}}| \\ |Q_b^{I_{tso}} - q_b^{I_{dso}}| \\ |V_b^{I_{tso}} - v_b^{I_{dso}}| \end{bmatrix} \leq \begin{bmatrix} \epsilon_p^{des} \\ \epsilon_q^{des} \\ \epsilon_v^{des} \end{bmatrix} \quad (58)$$

381 The process of solving the proposed coordination scheme is shown in Fig. 2. Based on this
 382 flowchart, the process starts with initializing the model parameters and defining the preferable degree
 383 of security (i.e. λ_{des}). Then, the TSO performs the following optimisation:

$$\min \{OF^{TSO}(X_{tso}^{DV})\} \quad (59)$$

Subject to :

$$H^{tso}(X_{tso}^{DV}) \leq 0 \quad (60)$$

$$G^{tso}(X_{tso}^{DV}) = 0 \quad (61)$$

384 where (59) is the TSO optimizer's objective function (i.e. (1)), and the constraints (60) and (61)
 385 represent all equality and inequality constraints of the transmission network (i.e. the constraints (4)-
 386 (25)). X_{tso}^{DV} represents the decision variables of the transmission network optimizer including those
 387 of the boundary points. The optimal solution of the boundary variables is reported to the DSO's
 388 distributed optimizers via (27)-(30). For any given transmission bus, the corresponding downstream
 389 distribution feeders are optimized based on (62)-(64) in a distributed manner.

$$\min \{OF^{DSO}(X_{dso}^{DV})\} \quad (62)$$

Subject to :

$$H^{dso}(X_{dso}^{DV}) \leq 0 \quad (63)$$

$$G^{dso}(X_{dso}^{DV}) = 0 \quad (64)$$

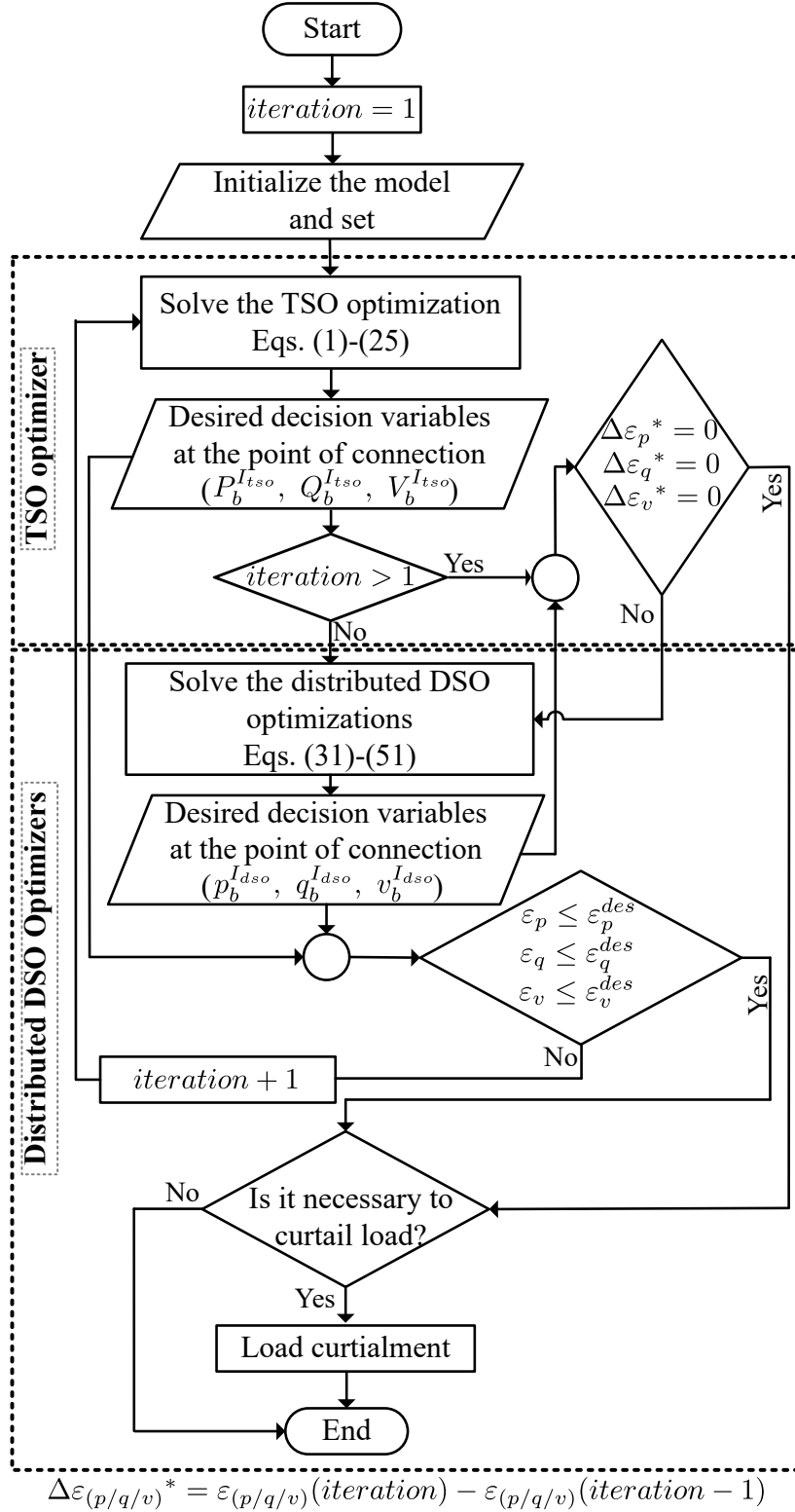


Figure 2: Flowchart of the proposed framework for TSO-DSO coordination.

390 where (62) is the objective function of the distribution network d and equations (63) and (64) are the
391 equality and inequality constraints of each distribution network (i.e. constraints (34)-(56)). X_{dso}^{DV} is
392 the set of decision variables for each distribution network. At the distribution level, each DSO applies

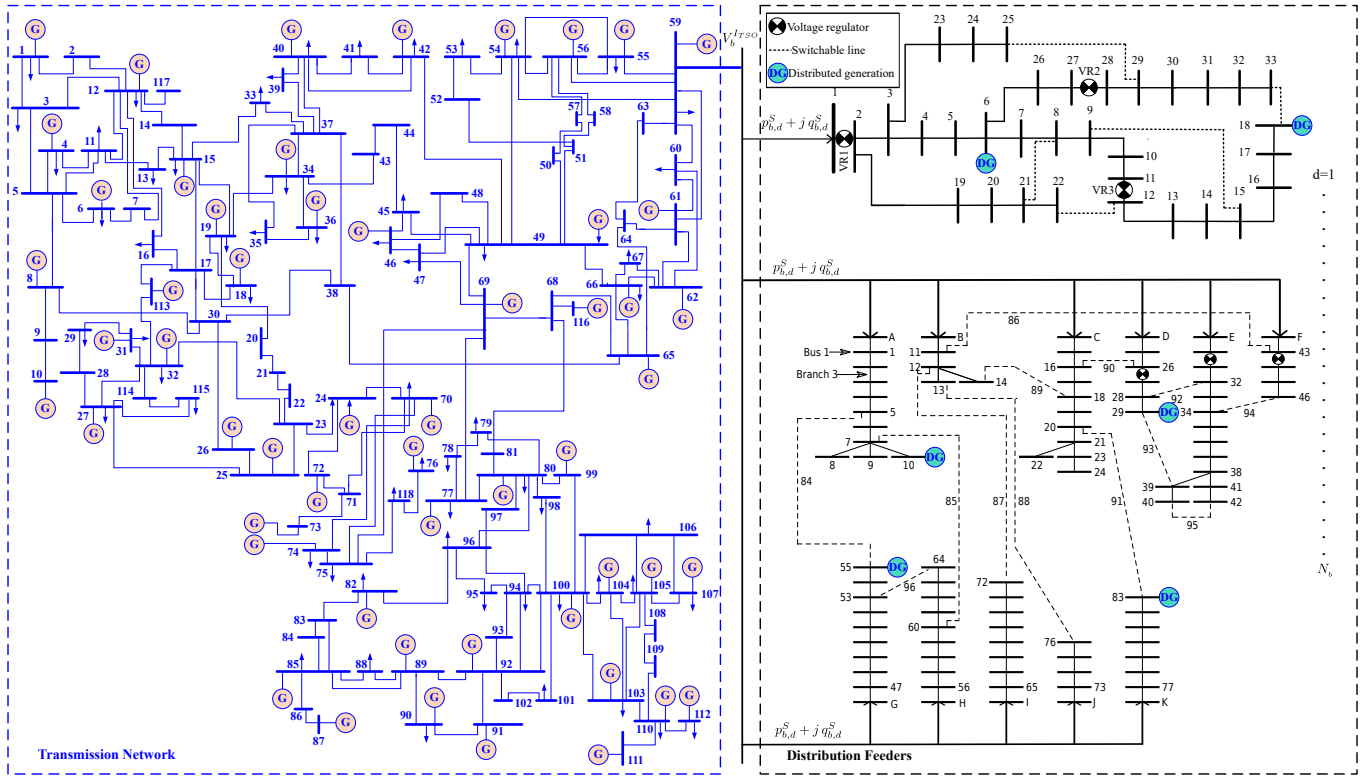


Figure 3: One-line diagram of the studied transmission and distribution networks.

393 its available flexibility measures in all feeders in a distributed manner to comply with the requirements
 394 of the TSO. While each DSO can provide a different degree of flexibility based on their capabilities,
 395 secure coordination is achieved if the convergence condition (i.e. (58)) is met.

396 If the convergence criterion is not met in the current iteration, the boundary set-points obtained
 397 by the DSO's distributed optimisers, are aggregated via (26) and sent back to the centralised TSO
 398 optimiser to set up the next iteration. The TSO then solves the optimisation in equations (59)-(61).
 399 From the second iteration, the TSO has the autonomy to check the desired values of set points in the
 400 point of connection. If the values of the boundary set-points obtained from the TSO are equal to those
 401 received from the previous iteration of the DSOs, it is not possible to apply further changes using the
 402 flexibility measures at the distribution level. At this point, the TSO sends the order to the DSOs to
 403 check for the load curtailment. The necessary load curtailment is then applied by the DSOs. In the
 404 first iteration and for the TSO's centralised optimiser, it is worth noting that , the DSOs' distributed
 405 optimisation models have not been solved yet, Eq. (3).

406 Conversely, if there is a difference between the set-points, the TSO allows the DSOs to perform
 407 their own distributed optimisations and utilise their flexibility measures to decrease load curtailment.
 408 This process is repeated by the TSO and distributed DSO optimisers until the convergence criterion is
 409 met or it is not possible to apply more adjustment to the set-points indicated by TSO.

410 5. Case study

411 The optimisation models in the TSO and DSO levels are non-linear programming and mixed-
 412 integer non-linear programming, respectively. Both models are implemented in general algebraic
 413 modelling system (GAMS) software [33]. In order to solve the MINLP problem, the DICOPT solver

414 considers two important solutions: (i) “best estimate”; (ii) “best integer”. The optimal bound of integer
 415 solution is provided by “best estimate”, while the best solutions of the problem which complies with
 416 the integer requirements is provided by “best integer”. In the solver algorithm, the quality of the opti-
 417 mal solution can be measured using a criterion which defines the distance between “best estimate” and
 418 the “best integer”, called “relative gap”. In the GAMS environment, this criterion is defined as “optcr”.
 419 The “optcr” defines the quality of the optimality of MIP master problems. The value of “optcr” is
 420 obtained as below [34]:

$$optcr = \frac{|best\ estimate - best\ integer|}{\max\{|best\ estimate| - |best\ integer|\}} \quad (65)$$

421 For example, if “best integer” =200 and the “best estimate” =250, the ”optcr”=0.20. For a large
 422 problem, the MIP solver can be stopped earlier by defining the value of ”optcr”. For instance if
 423 ”optcr”=0.20, the MIP solver is forced to stop as soon as the relative gap is less than 0.20. The
 424 value of ”optcr” is defined as zero in this paper so as to define an optimal solution which guarantees
 425 the quality of convergence degree. In this case, the solver does not stop until the distance between the
 426 best possible integer solution and the best found integer solution is zero.

427 The IEEE 118-bus system, here, is considered the test transmission network. The data of this
 428 system is available in [35]. The 83-bus practical distribution network of Taiwan Power Company [36]
 429 and the IEEE 33-bus distribution feeder [37] are considered as the sample downstream distribution
 430 networks. It is assumed that 8 parallel IEEE 33-bus distribution feeders and 5 parallel 83-bus Taiwan
 431 Power Company distribution networks are connected to Bus 59 of the IEEE 118-bus transmission
 432 system. This bus has the largest amount of load in the transmission network and is more likely to
 433 experience load shedding in case of an emergency condition (e.g. sudden load increase). The rest
 434 of the load in this bus, and other buses of the transmission network, are assumed as aggregated load
 435 in transmission level. The one-line diagram of IEEE 118-bus transmission network and connected
 436 distribution networks including the location of voltage regulators and potentially switchable lines in
 437 each feeder is shown in Fig. 3. The location of distributed generation (DG) units in distribution level is
 438 shown in this figure. The data of DGs is taken from [12].

439 The active and reactive power share of each distribution network (i.e., $\pi_{b,d}^p$ and $\pi_{b,d}^q$ in (27) and (29))
 440 is defined based on their total load. Therefore, the values of $\pi_{b,d}^p$ and $\pi_{b,d}^q$ are 0.178 and 0.156 for IEEE
 441 33-bus distribution feeders respectively, and they are respectively 0.822 and 0.844 for 83-bus Taiwan
 442 Power Company distribution networks. Moreover, $\epsilon_{(p/q/v)}^{des}$ are assumed to be 0.004 p.u in (58).
 443 Furthermore, w_1 and w_2 are both assumed to be 0.5 in (1) and (31), respectively. The share of various
 444 demand models, including the residential (R), commercial (C) and industrial (I) loads in exponential
 445 (EXP) load model is summarised in Table 2.

446 To analyse the effectiveness of the proposed TSO-DSO coordination scheme under an emergency
 447 condition, it is assumed that the transmission system’s load is increased by 10% (evenly in all buses).
 448 The desired security margin of the TSO-DSO coordination (i.e. λ_{des}) is taken to be 10%.

449 5.1. Flexibility with Network reconfiguration and CVR

450 The computational data of the proposed model is summarised in Table 3. The simulations are
 451 performed on an Intel(R) Core(TM) i5-6600 CPU 3.30GHz with 16 GB of RAM. Table 3 demonstrates
 452 that the proposed method achieved a considerable short computational time, in order of seconds. The
 453 distributed DSO optimisation models can be solved in a distributed manner via parallel computing.
 454 The convergence characteristics of the proposed TSO-DSO coordination model are shown in Fig. 4 for
 455 8 parallel IEEE 33-bus distribution feeders and 5 parallel 83-bus Taiwan Power Company distribution

Table 2
Various demands share in EXP load model.

Load model	ψ	$\alpha_{b,d}^\psi$	$\beta_{b,d}^\psi$	$kp_{\psi,b}$	$kq_{\psi,b}$
EXP	<i>R</i>	1.20	2.90	0.33	0.33
	<i>C</i>	0.99	3.50	0.33	0.33
	<i>I</i>	0.18	6.00	0.34	0.34

R: Residential, C: Commercial, I: Industrial and EXP: Exponential load model

Table 3
Computational size of the proposed TSO-DSO coordination model.

Parameter	TSO	DSO (33-bus)	DSO (83-bus)
# of model variables	8,398	808	2,022
# of model constraints	6,256	708	2,048
Total execution time [s]	36.19	1.28	2.25

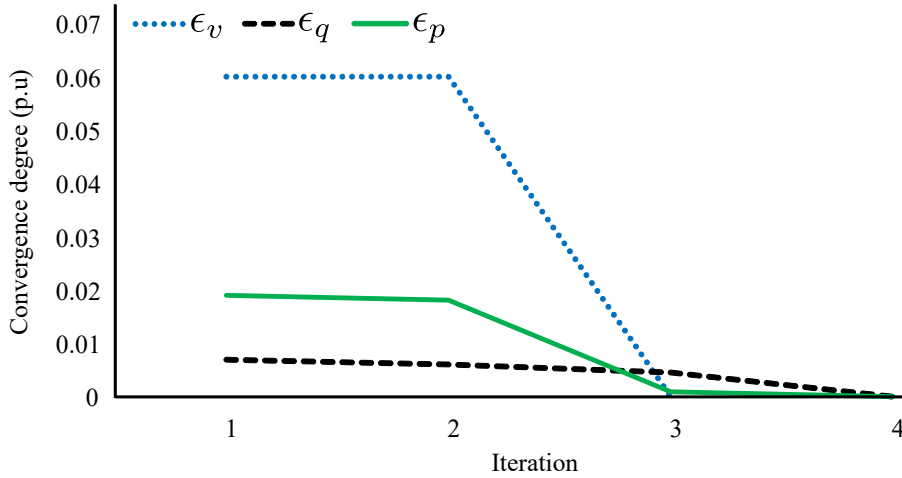


Figure 4: The convergence characteristics of the TSO-DSO coordination model for $N_b = 13$ and $\lambda_{des} = 10\%$.

456 networks connected to Bus 59 and the security margin of 10%. It can be seen that the proposed
457 decentralised TSO-DSO coordination model converges in a few iteration (e.g. four iterations for $\lambda_{des} =$
458 10%). Moreover, voltage at the interface point is converged even faster, such that $\epsilon_v \leq \epsilon_v^{des}$ after three
459 iterations. Having the voltage regulators in distribution feeders enables more flexibility in both active and
460 reactive power demands to enhance the convergence degree of the proposed framework.

461 Figure 5 shows the changes in the optimal value of load curtailment for different number of dis-
462 tribution networks connected to the Bus 59, and different levels of the security margin. The main
463 observations based on this figure are:

- 464 1. Number of parallel distribution networks (i.e. N_b): it can be seen from Figs. 5-(a)-(c) that
465 increasing the number of connected distribution networks can reduce the number of iterations.
466 Increasing the number of distribution networks raises the degree of flexibility and contribution
467 in the load reduction. The optimisation achieved the desired convergence degree in two iteration
468 for $N_b = 13$. Also, this factor can influence the load curtailment. For example, in Fig. 5-(b),
469 the total amount of load curtailment for the distributed DSO optimisers is zero for $N_b^{33bus} = 15$
470 and $N_b^{33bus} = 13$, while it is 0.14 MW for $N_b^{33bus} = 7$. The value of actual load curtailment is

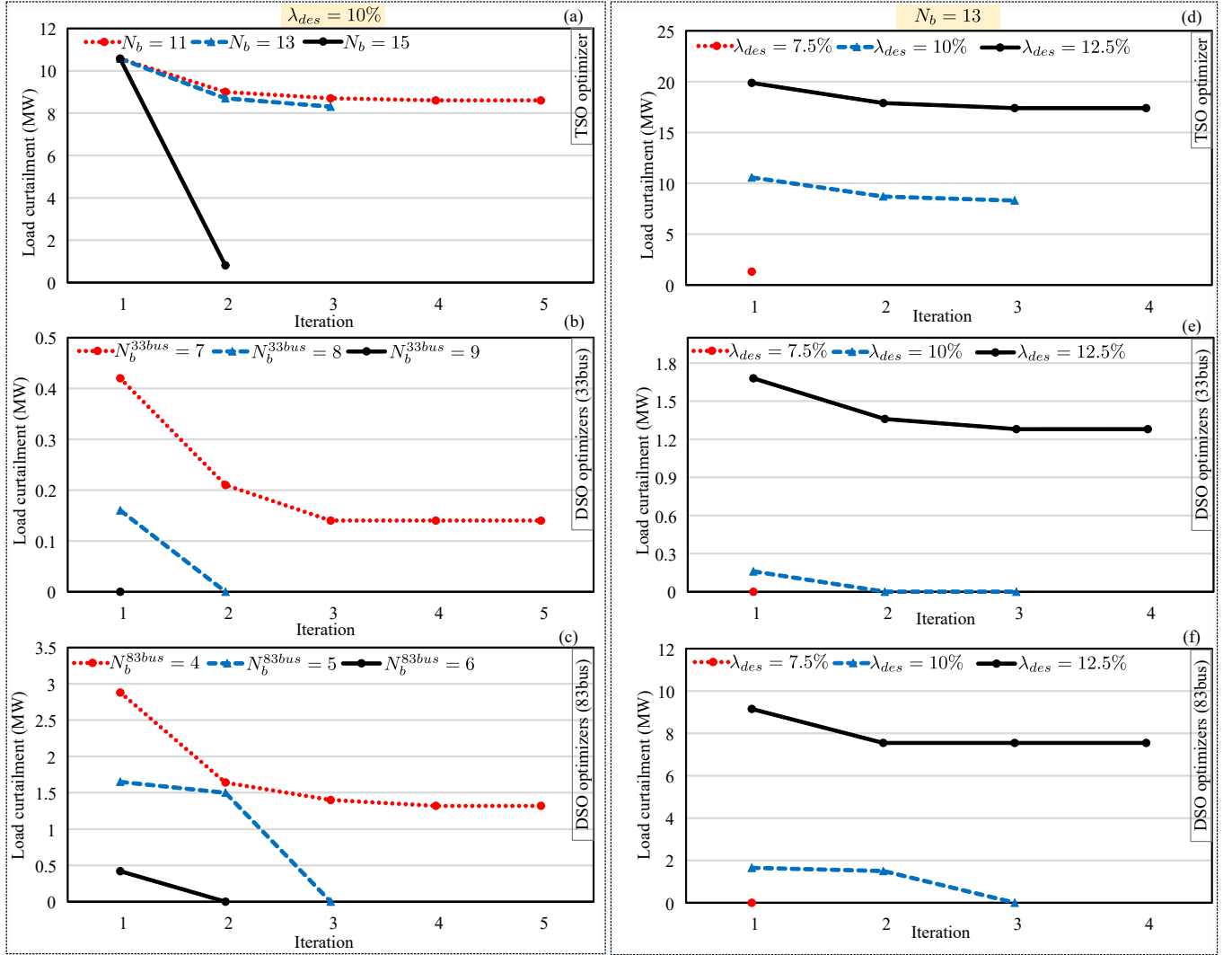


Figure 5: Load curtailment for different values of N_b and λ_{des} : (a)-(c) TSO and DSO optimisers' results for $\lambda_{des} = 10\%$ and different values of N_b , (d)-(f) TSO and DSO optimisers' results for $N_b = 13$ and different security margins.

- 471 1.32 MW in 83-bus distribution network for $N_b^{83bus} = 4$. This means that the actual value of
472 load curtailment increases for the larger distribution networks.
- 473 2. The role of distributed flexibility measures: these techniques play a crucial role in decreasing the
474 load curtailment in the distribution networks. For instance, for $N_b = 11$ in Fig 5-(a), although the
475 TSO requested 8.6 MW load curtailment in the TSO-DSO interface, the distribution network
476 optimisers only curtailed 0.14 MW and 1.32 MW in Figs. 5-(b) and 5-(c) respectively. This
477 means that $8.6 - (1.32 + 0.14) = 7.0$ MW (i.e. 81%) of the requested load curtailment by the
478 TSO is handled via the available flexibility measures, namely feeder reconfiguration and conser-
479 vation voltage reduction. It is worth mentioning that no physical load curtailment is realized by
480 the DSO optimisers for $N_b = 13$ and $N_b = 15$.
- 481 3. Security margin (i.e. λ_{des}): this transmission-level parameter has a significant impact on the
482 load curtailment. Increasing the security margin from 10% to 12.5% in Fig. 5-(d) doubles the
483 amount of required load curtailment by the TSO optimiser in the boundary point (i.e. Bus 59).

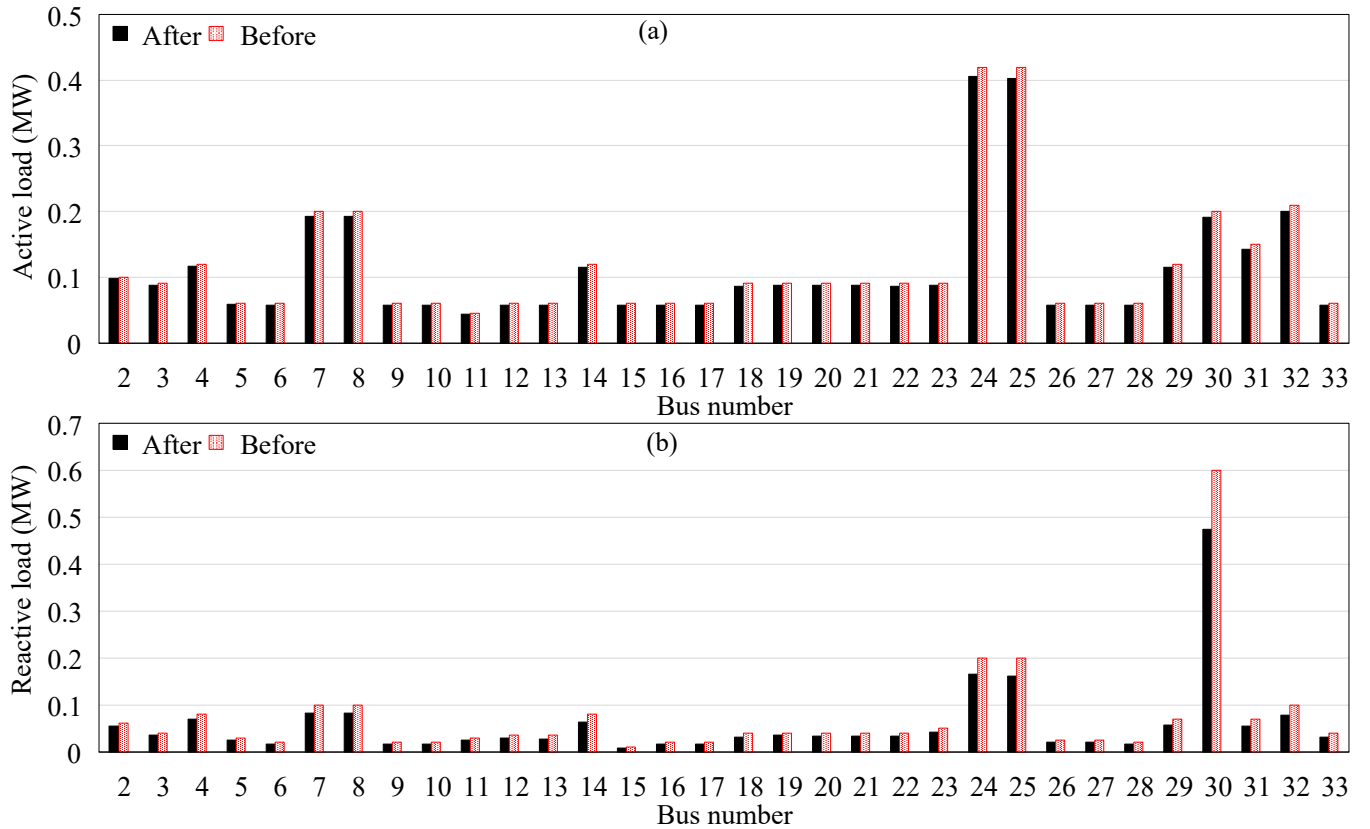


Figure 6: Nodal demand values in IEEE 33-bus distribution feeder before and after applying the flexibility measures (for $N_b = 13$ and $\lambda_{des} = 10\%$): (a) active power, (b) reactive power.

484 Additionally, one can observe from Figs. 5-(e) and 5-(f) the higher the λ_{des} the more the actual
 485 load curtailment by DSO. Moreover, this measure also influences the number of iterations for
 486 achieving desired convergence degree.

487 4. Secure coordination: in Figs. 5-(e) and 5-(f), since the TSO optimiser has not observed any
 488 changes in the interface set-points from iteration 3 to 4 for $\lambda_{des} = 12.5\%$, the DSO optimisers
 489 observed load curtailment in iteration 3 for maintaining the desired security margin over the
 490 whole system.

491 Active and reactive power of an IEEE 33-bus distribution network connected to Bus 59 before
 492 and after applying the flexibility measures is shown in Fig. 6. It is observed that the flexibility mea-
 493 sures reduce the active and reactive loads, especially for high demanded buses. The total active and
 494 reactive power of each distribution feeder before applying the flexibility measures are $3.72 MW$ and
 495 $2.30 MVAr$ respectively, while after applying the CVR and feeder reconfiguration the net active and
 496 reactive demands of each feeder decrease to $3.57 MW$ and $1.86 MVAr$, respectively. This means
 497 that each distribution network is capable of reducing its active and reactive demands by $0.14 MW$
 498 (i.e. 3.8% of total active power demand) and $0.43 MVAr$ (i.e. 19% of total reactive power demand),
 499 respectively, without any need for actual load curtailment (as also shown in Fig. 5-(b) for $N_b^{33bus} = 8$
 500 and $\lambda_{des} = 10\%$). For the 83-bus Taiwan Power Company distribution network, 2.6% and 14.2% of
 501 active and reactive power is compensated by the distribution flexibilities without the need for physical
 502 load curtailment (as also shown in Fig. 5-(c) for $N_b^{83bus} = 5$ and $\lambda_{des} = 10\%$).

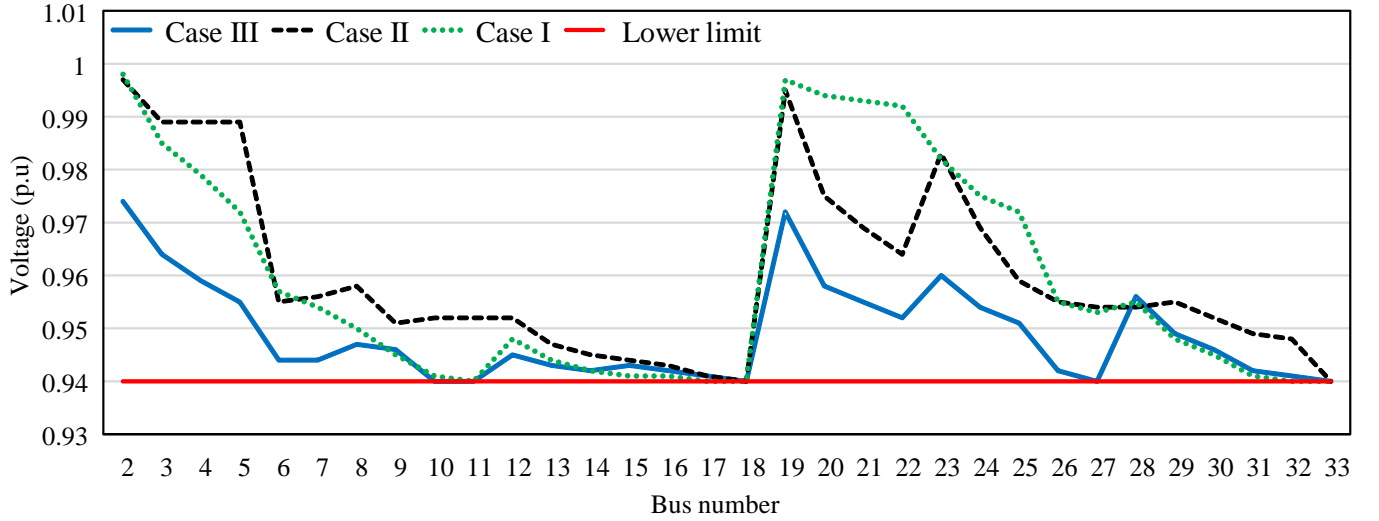


Figure 7: Optimal value of voltage magnitude in the IEEE 33-bus distribution network for different case studies (for $N_b = 13$ and $\lambda_{des} = 10\%$).

503 Figure 7 investigates the voltage profile obtained by the distributed DSO optimisers for a specific
 504 feeder connected to bus 59 in the following three cases:

- 505 • **Case I:** With CVR and without feeder reconfiguration;
- 506 • **Case II:** Without CVR and with feeder reconfiguration;
- 507 • **Case III:** With both CVR and feeder reconfiguration.

508 This figure shows that solely using CVR (i.e. *Case I*) decreases the voltage level in the end buses
 509 to the corresponding lower limit. In *Case II*, however, just feeder reconfiguration has resulted in better
 510 values of voltage level across the feeder. In *Case III*, where both CVR and feeder reconfiguration are
 511 considered as the flexibility measures, the voltage level is reduced in a coordinated manner to satisfy
 512 the demand reduction forced by the TSO. The active and reactive demands, in this case, have already
 513 been shown in Fig. 6.

514 Moreover, for $N_b = 13$ and $\lambda_{des} = 10\%$, the overall active power curtailment in all distribution
 515 networks in cases *I*, *II* and *III* is 3.6 MW, 2.4 MW, and 0.0 MW, respectively. Although each of
 516 the CVR and feeder reconfiguration flexibilities can individually decrease the actual load curtailment,
 517 their coordinated utilisation is a better practice for reducing the load curtailment in the TSO-DSO
 518 coordination process.

519 Finally, the effect of security margin on the voltage regulators' settings as well as the optimal
 520 configuration of each sample distribution feeder are shown in Figs. 8 and 9, respectively. Figure
 521 8 demonstrates that how the tap setting is changed for voltage regulators to cope with the TSO's
 522 requirements in terms of the desired security margin. For example, the voltage regulator installed on
 523 the line between buses 1 and 2 (i.e., VR1) changes its tap by 5% in order to cope with a 2.5% rise in the
 524 security margin. These results can also be seen in Fig. 9, where the distribution feeder's configuration
 525 is changed for different values of λ_{des} . Note that the radial configuration is preserved for all security
 526 margins.

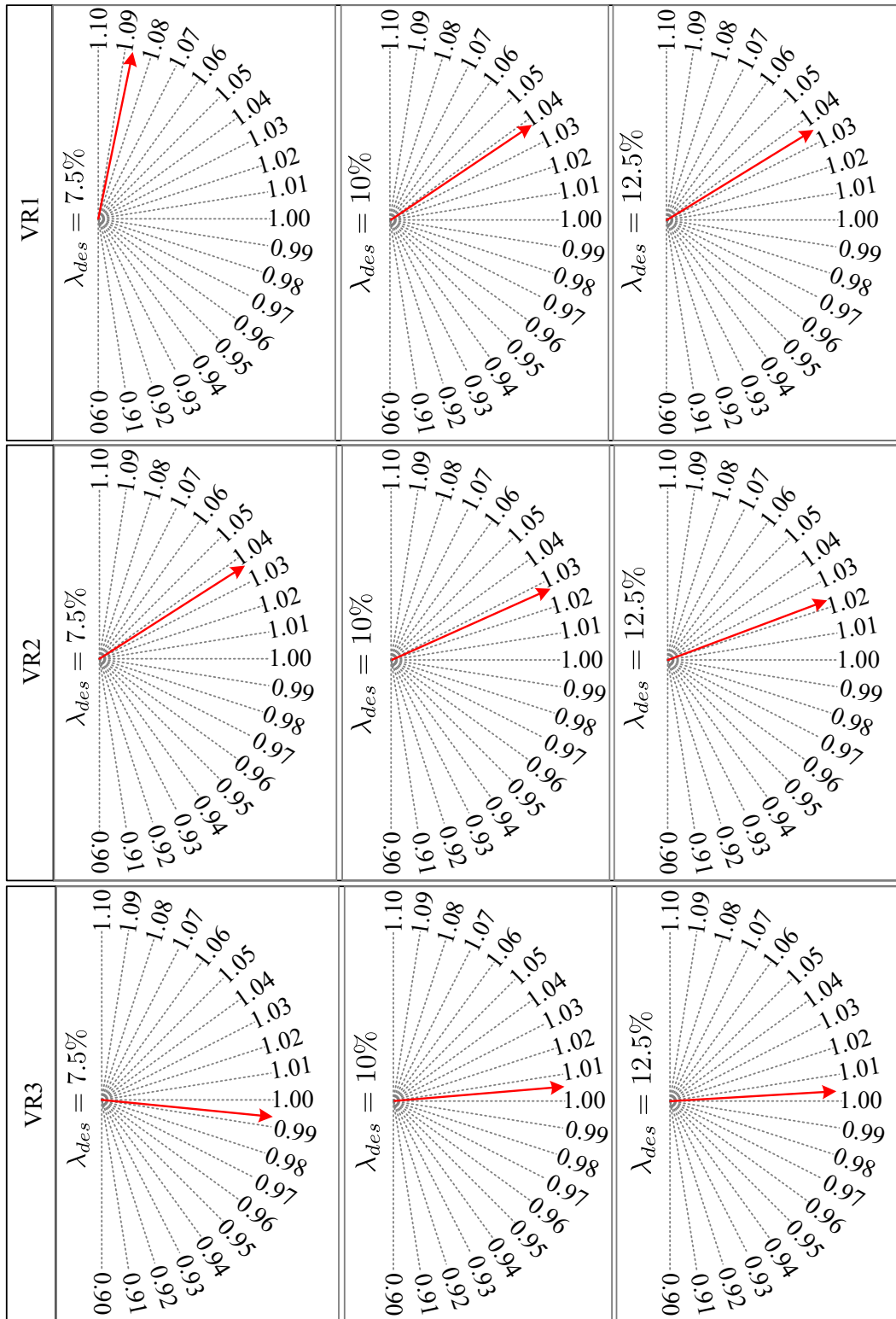


Figure 8: The optimal setting of voltage regulators installed in the IEEE 33-bus distribution network for different values of security margin and $N_b = 13$.

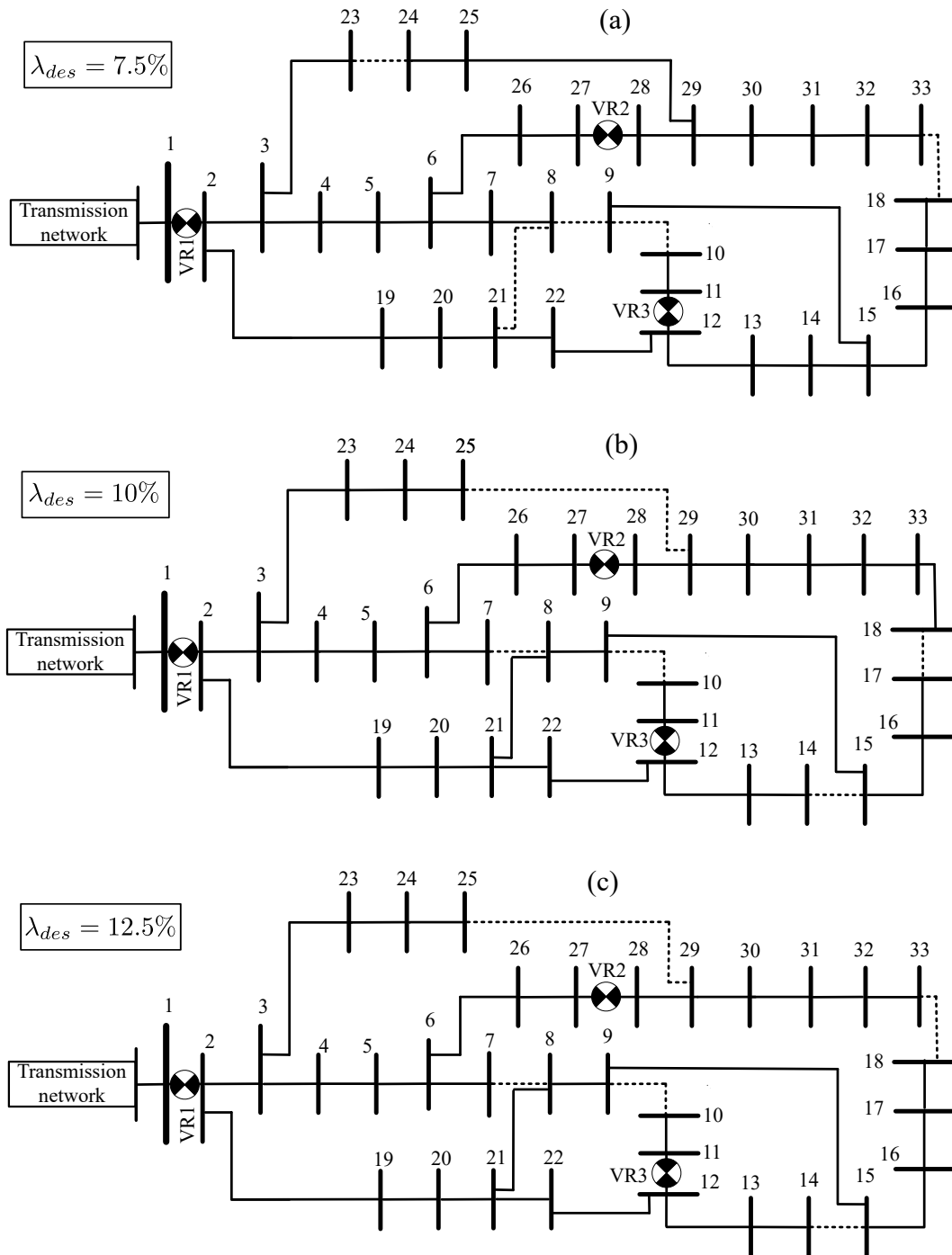


Figure 9: Variation of the IEEE 33-bus distribution network configuration for different values of security margin and $N_b = 13$.

527 *5.2. Value of DER flexibility*

528 This section evaluates the effectiveness of DERs in providing flexibility services for the TSO-DSO
 529 coordination. As shown in Fig. 3, a number of DGs are installed in the distribution network and their
 530 effect on decreasing the needs for load curtailment in the emergency condition is analysed.

531 The simulation result shows that the coordination with the IEEE 33-bus distribution network con-
 532 verges in one iteration and the value of load shedding is zero with the DGs in the system; the 83-bus

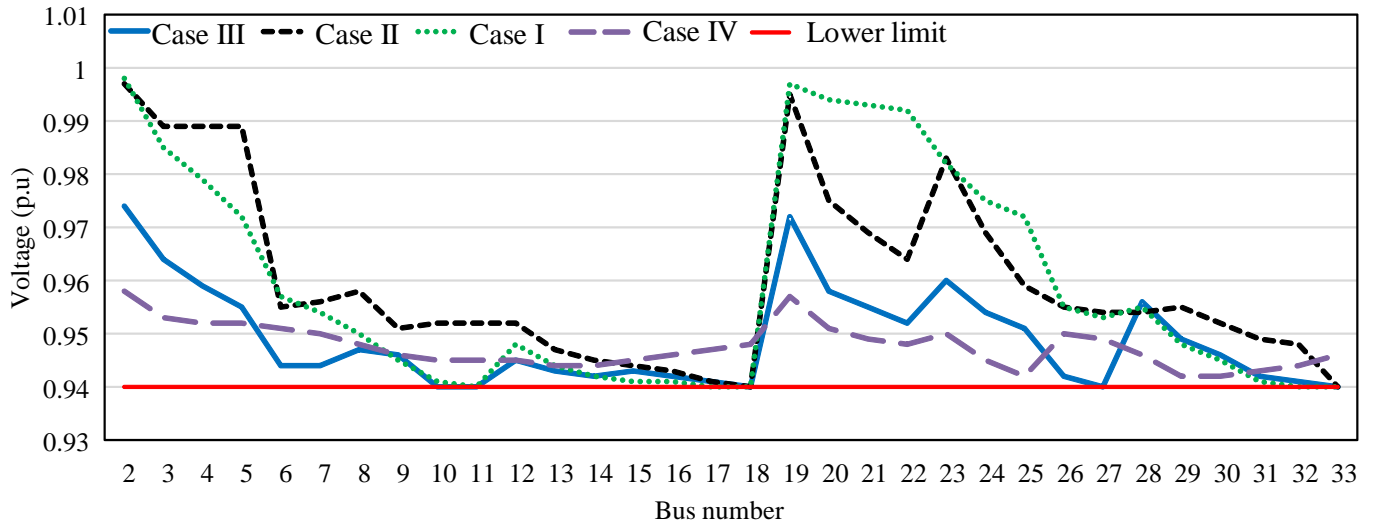


Figure 10: Optimal value of voltage magnitude in the IEEE 33-bus distribution network for different case studies with consideration for the DER effect (for $N_b = 13$ and $\lambda_{des} = 10\%$).

533 Taiwan Power Company distribution networks converges after two iteration, also with zero load shed-
 534 ding. This results show the importance of DERs in decreasing the needs for extra communication be-
 535 tween DSO and TSO, while achieving zero load shedding. Therefore, optimal coordination of DERs
 536 is an efficient method in achieving the secure TSO-DSO coordination.

537 In order to evaluate the effect of DERs on voltage profile, the case studies described in Fig. 7 are
 538 compared against a case study with DERs, network reconfiguration and CVR (called Case IV). The
 539 result of this comparison is given in Fig. 10. It can be seen from this figure that the combination of
 540 distributed flexibility methods with DERs provides better threshold for the voltage profile, without the
 541 need for load curtailment.

542 Also, the optimal setting of voltage regulators in Case III and Case IV are compared in Fig. 11.
 543 This figure shows that adding the DERs decreased the need for higher level of tap changing in the
 544 voltage regulators. This means the local generation decreases the need for higher contribution from the
 545 loads in complying with the security measures of the TSO-DSO coordination.

546 Finally, to evaluate the effect of linking multiple transmission network buses, IEEE 33-bus distri-
 547 bution networks are connected to Bus 59 while 83-bus Taiwan Power Company distribution networks
 548 are connected to Bus 116 of transmission network. Fig. 12. It can be seen from this figure that the
 549 DER flexibility can provide the required flexibility without the need for the load curtailment. Although
 550 network reconfiguration and CVR provided considerable value of flexibility, some load curtailment still
 551 happened in this case.

552 6. Conclusion

553 The transformation of power systems towards integrated networks of different entities in which
 554 distribution and transmission system operators cooperate together towards a coordinated TSO-DSO
 555 scheme is a promising development. This scheme enables traditionally passive distribution networks
 556 to be active entities of such coordination. However, the challenge of voltage security and distributed
 557 flexibilities provided by DSOs for keeping the whole system in the desired loading margin needs fur-
 558 ther investigations. This paper highlights the distributed flexibility measures for preserving the voltage

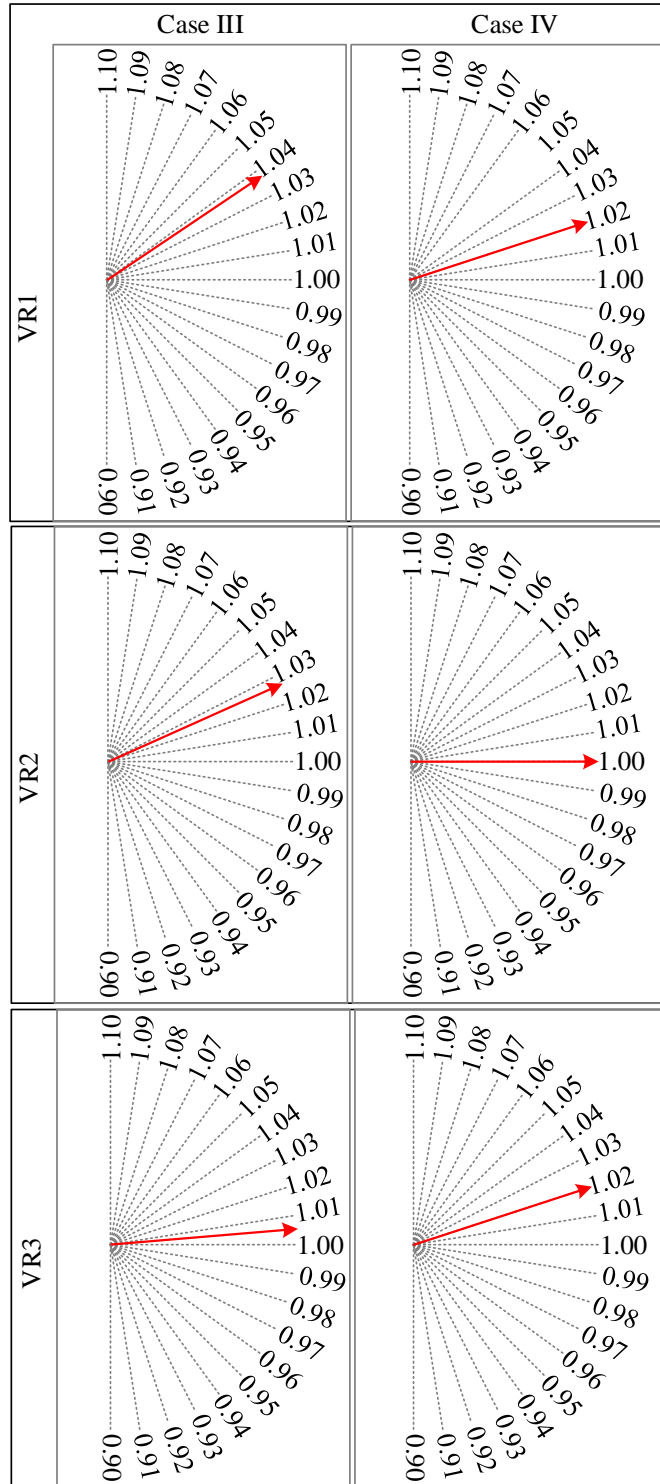


Figure 11: The optimal setting of voltage regulators installed in the IEEE 33-bus distribution network for cases III and IV (for $N_b = 13$ and $\lambda_{des} = 10\%$).

559 security margin of the TSO-DSO coordination approach via a decentralised optimisation framework.
 560 At the transmission level, the centralised TSO optimizer aims at minimising the load curtailment in
 561 the heavily loaded transmission network buses to preserve the required security margin under a con-
 562 tingency condition (i.e. sudden increase in the system load). The optimal set-points of transmission

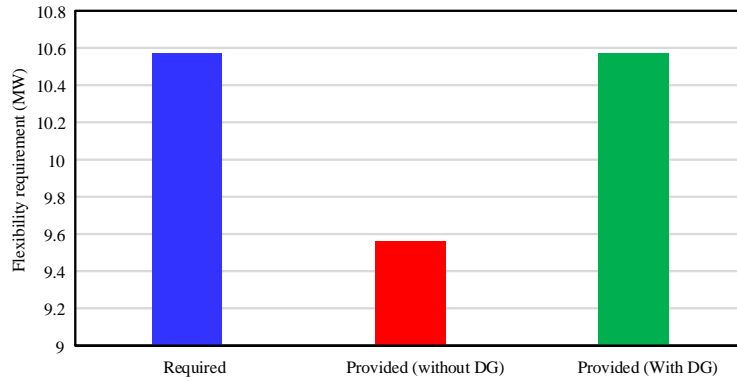


Figure 12: Optimal value of flexibility provided when IEEE 33-bus distribution networks are connected to Bus 59 while 83-bus Taiwan Power Company distribution networks are connected to Bus 116.

563 buses in terms of active/reactive power and voltage level, are determined by this optimisation model
 564 and sent to the downstream distribution networks at the point of connection between these grids. At the
 565 distribution level, the distributed optimisers of DSOs aim at minimising the difference between their
 566 set-points and the corresponding values sent by the TSO in the TSO-DSO boundary points as well as
 567 physical load curtailment, simultaneously. To achieve these goals with minimum unavoidable load cur-
 568 tailment, DSOs utilise their distributed flexibilities such as conservation voltage reduction and feeder
 569 reconfiguration. The efficiency of these flexibility methods is evident in the results. These distributed
 570 flexibility measures compensated 81% of load curtailment requested by the TSO. This result shows the
 571 importance of benefiting from flexibility measures in the distribution networks, highlighting their role
 572 as an active player in the TSO-DSO coordination. The results show that the number of distribution
 573 feeders available in the DSO distributed optimisers can reduce both the actual load curtailment and
 574 the number of iterations for the TSO-DSO coordination. This means that the proposed framework can
 575 achieve short computational time, in order of seconds, when the number of distribution networks is
 576 increased. According to the results, it can be concluded that:

- 577 • The coordinated utilization of CVR and feeder reconfiguration is a promising option for the
 578 reduction of physical load curtailment in the TSO-DSO coordination process. Joint utilisation
 579 of CVR and feeder reconfiguration reduced the need for curtailing the active and reactive load
 580 in each individual distribution network by 3.8% and 19% respectively. These methods can be
 581 utilised along with DER flexibility options in the future studies to guarantee system security.
- 582 • Increasing the security margin raises the required load curtailment by the TSO and consequently
 583 the actual load curtailment by DSOs. Increasing the security margin by 2.5% resulted in a
 584 twofold increase in the required load curtailment by the TSO. This criteria is important in the
 585 coordination schemes that require a higher level of security. Under such paradigm, the system
 586 operators need to curtail load to preserve higher security margins.
- 587 • A 2.5% increase in the security margin requires 5% change in the tap settings of voltage reg-
 588 ulators installed in the distribution networks. This shows the effect of security margin in the
 589 transmission level on the flexibility measures taken by DSOs. It also highlights the active role of
 590 distributed flexibilities in preserving the whole system security.

591 References

- 592 [1] J. Bialek, “What does the GB power outage on 9 august 2019 tell us about the current state of
593 decarbonised power systems?,” Energy Policy, vol. 146, p. 111821, 2020.
- 594 [2] H. Sun, Q. Guo, J. Qi, V. Ajjarapu, R. Bravo, J. Chow, Z. Li, R. Moghe, E. Nasr-Azadani,
595 U. Tamrakar, et al., “Review of challenges and research opportunities for voltage control in smart
596 grids,” IEEE Transactions on Power Systems, vol. 34, no. 4, pp. 2790–2801, 2019.
- 597 [3] H. Brunner, and A. Zegers, “An overview of current interaction between transmission and distri-
598 bution system operators and an assessment of their cooperation in smart grids.”
- 599 [4] A. G. Givisiez, K. Petrou, and L. F. Ochoa, “A review on tso-dso coordination models and solution
600 techniques,” Electric Power Systems Research, vol. 189, p. 106659, 2020.
- 601 [5] Global Power System Transformation, “Inaugural research agenda.”
- 602 [6] M. Kalantar-Neyestanaki, F. Sossan, M. Bozorg, and R. Cherkaoui, “Characterizing the reserve
603 provision capability area of active distribution networks: A linear robust optimization method,”
604 IEEE Transactions on Smart Grid, vol. 11, no. 3, pp. 2464–2475, 2019.
- 605 [7] S. Stanković and L. Söder, “Probabilistic reactive power capability charts at dso/tso interface,”
606 IEEE Transactions on Smart Grid, vol. 11, no. 5, pp. 3860–3870, 2020.
- 607 [8] P. Sheikahmadi, S. Bahramara, A. Mazza, G. Chicco, and J. P. Catalão, “Bi-level optimiza-
608 tion model for the coordination between transmission and distribution systems interacting with
609 local energy markets,” International Journal of Electrical Power & Energy Systems, vol. 124,
610 p. 106392, 2021.
- 611 [9] V. A. Evangelopoulos, I. I. Avramidis, and P. S. Georgilakis, “Flexibility services management
612 under uncertainties for power distribution systems: Stochastic scheduling and predictive real-time
613 dispatch,” IEEE Access, vol. 8, pp. 38855–38871, 2020.
- 614 [10] C. Lin, W. Wu, and M. Shahidehpour, “Decentralized ac optimal power flow for integrated trans-
615 mission and distribution grids,” IEEE Transactions on Smart Grid, vol. 11, no. 3, pp. 2531–2540,
616 2019.
- 617 [11] G. C. Kryonidis, M. E. Tsampouri, K.-N. D. Malamaki, and C. S. Demoulias, “Distributed
618 methodology for reactive power support of transmission system,” Sustainable Energy, Grids and
619 Networks, p. 100753, 2022.
- 620 [12] T. Jiang, C. Wu, R. Zhang, X. Li, H. Chen, and G. Li, “Flexibility clearing in joint energy and
621 flexibility markets considering tso-dso coordination,” IEEE Transactions on Smart Grid, 2022.
- 622 [13] F. Marten, L. Löwer, J.-C. Töbermann, and M. Braun, “Optimizing the reactive power balance
623 between a distribution and transmission grid through iteratively updated grid equivalents,” in
624 2014 Power Systems Computation Conference, pp. 1–7, IEEE, 2014.
- 625 [14] L. Kristov, P. De Martini, and J. D. Taft, “A tale of two visions: Designing a decentralized
626 transactive electric system,” IEEE Power and Energy Magazine, vol. 14, no. 3, pp. 63–69, 2016.

- 627 [15] Z. Yuan and M. R. Hesamzadeh, "Hierarchical coordination of tso-dso economic dispatch consid-
628 ering large-scale integration of distributed energy resources," Applied energy, vol. 195, pp. 600–
629 615, 2017.
- 630 [16] K. Purchala, L. Meeus, D. Van Dommelen, and R. Belmans, "Usefulness of dc power flow for
631 active power flow analysis," in IEEE Power Engineering Society General Meeting, 2005, pp. 454–
632 459, IEEE, 2005.
- 633 [17] A. Mohammadi, M. Mehrtash, and A. Kargarian, "Diagonal quadratic approximation for decen-
634 tralized collaborative tso+ dso optimal power flow," IEEE Transactions on Smart Grid, vol. 10,
635 no. 3, pp. 2358–2370, 2018.
- 636 [18] J. Silva, J. Sumaili, R. J. Bessa, L. Seca, M. A. Matos, V. Miranda, M. Caujolle, B. Goncer,
637 and M. Sebastian-Viana, "Estimating the active and reactive power flexibility area at the tso-dso
638 interface," IEEE Transactions on Power Systems, vol. 33, no. 5, pp. 4741–4750, 2018.
- 639 [19] S. Nikkhah, M.-A. Nasr, and A. Rabiee, "A stochastic voltage stability constrained ems for
640 isolated microgrids in the presence of pevs using a coordinated uc-opf framework," IEEE
641 Transactions on Industrial Electronics, vol. 68, no. 5, pp. 4046–4055, 2020.
- 642 [20] A. Sarhan, V. K. Ramachandaramurthy, T. S. Kiong, and J. Ekanayake, "Definitions and di-
643 mensions for electricity security assessment: A review," Sustainable Energy Technologies and
644 Assessments, vol. 48, p. 101626, 2021.
- 645 [21] Z. Li, Q. Guo, H. Sun, J. Wang, Y. Xu, and M. Fan, "A distributed transmission-distribution-
646 coupled static voltage stability assessment method considering distributed generation," IEEE
647 Transactions on Power Systems, vol. 33, no. 3, pp. 2621–2632, 2017.
- 648 [22] A. O. Rousis, D. Tzelepis, Y. Pipelzadeh, G. Strbac, C. D. Booth, and T. C. Green, "Provision of
649 voltage ancillary services through enhanced tso-dso interaction and aggregated distributed energy
650 resources," IEEE Transactions on Sustainable Energy, vol. 12, no. 2, pp. 897–908, 2020.
- 651 [23] K. Tang, M. Ge, S. Dong, J. Cui, and X. Ma, "Transmission contingency analysis based on data-
652 driven equivalencing of radial distribution networks considering uncertainties," IEEE Access,
653 vol. 8, pp. 227247–227254, 2020.
- 654 [24] A. Bachouris, C. Kaskouras, G. Papaioannou, and M. Sousounis, "Tso/dso coordination for
655 voltage regulation on transmission level: A greek case study," in 2021 IEEE Madrid PowerTech,
656 pp. 1–7, IEEE, 2021.
- 657 [25] S. Karagiannopoulos, C. Mylonas, P. Aristidou, and G. Hug, "Active distribution grids providing
658 voltage support: The swiss case," IEEE Transactions on Smart Grid, vol. 12, no. 1, pp. 268–278,
659 2020.
- 660 [26] F. Escobar, J. M. Viquez, J. García, P. Aristidou, and G. Valverde, "Coordination of ders and
661 flexible loads to support transmission voltages in emergency conditions," IEEE Transactions on
662 Sustainable Energy, vol. 13, no. 3, pp. 1344–1355, 2022.
- 663 [27] A. Nawaz, H. Wang, Q. Wu, and M. Kumar Ochani, "Tso and dso with large-scale distributed
664 energy resources: A security constrained unit commitment coordinated solution," International
665 Transactions on Electrical Energy Systems, vol. 30, no. 3, p. e12233, 2020.

- 666 [28] S. Lefebvre, G. Gaba, A. Ba, D. Asber, A. Ricard, C. Perreault, and D. Chartrand, "Measuring the
667 efficiency of voltage reduction at hydro-québec distribution," in 2008 IEEE Power and Energy
668 Society General Meeting-Conversion and Delivery of Electrical Energy in the 21st Century,
669 pp. 1–7, IEEE, 2008.
- 670 [29] P. Harsh and D. Das, "Energy management in microgrid using incentive-based demand response
671 and reconfigured network considering uncertainties in renewable energy sources," Sustainable
672 Energy Technologies and Assessments, vol. 46, p. 101225, 2021.
- 673 [30] E. Leonidaki, D. Georgiadis, and N. Hatziargyriou, "Decision trees for determination of opti-
674 mal location and rate of series compensation to increase power system loading margin," IEEE
675 Transactions on Power Systems, vol. 21, no. 3, pp. 1303–1310, 2006.
- 676 [31] M. E. Baran and F. F. Wu, "Network reconfiguration in distribution systems for loss reduction
677 and load balancing," IEEE Power Engineering Review, vol. 9, no. 4, pp. 101–102, 1989.
- 678 [32] M. Lavorato, J. F. Franco, M. J. Rider, and R. Romero, "Imposing radiality constraints in dis-
679 tribution system optimization problems," IEEE Transactions on Power Systems, vol. 27, no. 1,
680 pp. 172–180, 2011.
- 681 [33] A. Soroudi, Power system optimization modeling in GAMS, vol. 78. Springer, 2017.
- 682 [34] I. E. Grossmann, J. Viswanathan, A. Vecchiotti, R. Raman, E. Kalvelagen, et al., "Gams/dicopt:
683 A discrete continuous optimization package," GAMS Corporation Inc, vol. 37, p. 55, 2002.
- 684 [35] R. D. Zimmerman, C. E. Murillo-Sánchez, and R. J. Thomas, "Matpower: Steady-state opera-
685 tions, planning, and analysis tools for power systems research and education," IEEE Transactions
686 on power systems, vol. 26, no. 1, pp. 12–19, 2010.
- 687 [36] C.-T. Su, C.-F. Chang, and J.-P. Chiou, "Distribution network reconfiguration for loss reduction
688 by ant colony search algorithm," Electric power systems research, vol. 75, no. 2-3, pp. 190–199,
689 2005.
- 690 [37] S. Nikkhah, I. Sarantakos, N.-M. Zografou-Barredo, A. Rabiee, A. Allahham, and D. Giaouris, "A
691 joint risk and security constrained control framework for real-time energy scheduling of islanded
692 microgrids," IEEE Transactions on Smart Grid, 2022.